Numerical Study of the Wet-season Hydrodynamics of a Macrotidally forced Bay with Complex Topography: Collier Bay, Kimberley, Western Australia

W. Zhou[1, 2, 3], A. Espinosa-Gayosso[1, 2, 3], N.L. Jones[1, 2, 3], and M. R. Hipsey[2, 3, 4]

[1] School of Civil, Environmental and Mining Engineering, University of Western Australia, Western Australia 6009, Australia

[2] UWA Ocean Institute, University of Western Australia, Western Australia 6009, Australia

[3] Western Australian Marine Science Institution, University of Western Australia, Western Australia 6009, Australia

[4] School of Earth and Environment, University of Western Australia, Western Australia 6009, Australia

Abstract

The Regional Ocean Modeling System (ROMS) was employed to study the wet season hydrodynamics of Collier Bay in the Kimberley region of Western Australia. Hydrodynamics of this semi-enclosed estuary is characterized by complex topography, macro-tides and highly seasonal freshwater inflow pulses. Freshwater inflows result in both horizontal and vertical density stratification. Tidally forced residual currents are much stronger around the islands and reefs, which is consistent with the complex topography. To study the interactive role of tides and freshwater inflows in determining the mass exchange in Collier Bay, Eulerian salt-flux decomposition and isohaline salt-flux decomposition are applied to a group of cross-sections distributed longitudinally from the river mouth to the open ocean. The Eulerian method decomposes the salt flux into three components to demonstrate the contribution of advection, exchange flow and tide-correlated flow to the net salt fluxes; the isohaline method provides more details about the salinity ranges of the downgradient and the upgradient components. Results show that bathymetric variation in different directions has different impacts on the interaction between tides and freshwater inflow in shaping salt fluxes and thus the horizontal mass exchange, which is helpful regarding a better understanding of the sediment and nutrient transport processes in this area.

Introduction

Collier Bay is an embayment located in the Kimberley region of Western Australia that is characterized by extreme tides, complex topography and a distinctive wet/dry-season climate. The tidal range is one of the largest in the world, reaching 10 m at spring tide (Cresswell and Badcock, 2000). The Kimberley region experiences a tropical monsoon cycle that consists of a dry season from May to October and a wet season from November to April. Average rainfall in the dry season is about 5% of the total annual rainfall (1440 mm/year), and the rest is concentrated in the wet season (Jones et al., 2014); consequently the freshwater inflow is highly seasonal. In turn, the stratification in Collier Bay shifts from weakly stratified in the dry season to strongly stratified in the wet season as stronger salinity gradients are established in both the horizontal and vertical directions by the large freshwater inflows. Water exchange and mass transport between the shallower inshore water in Collier Bay and the deeper offshore water occurs through three channels separated by islands and reefs, however, it remains unclear how the tides, topography and inflows interact to shape the net mass flux.

Here we demonstrate the role of the complex topography in determining the horizontal mass exchange at Collier Bay in the wet-season using results from the numerical model ROMS, validated against relevant oceanographic data. The analysis applies a Eulerian salt-flux decomposition and isohaline salt-flux decomposition approach to a group of cross-sections distributed longitudinally from the river mouth to the open ocean (Figure 1).

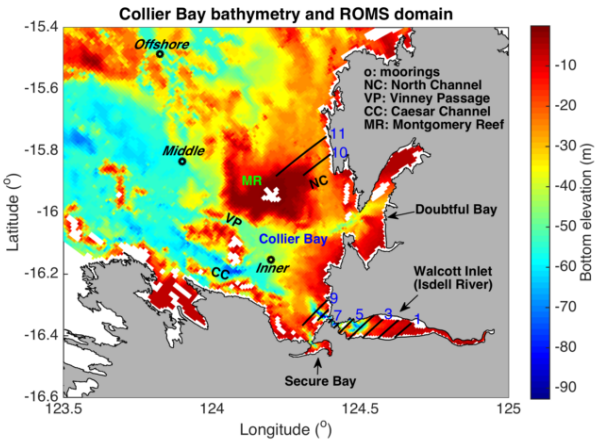

Figure 1. Collier Bay bathymetry and ROMS domain. The short solid lines are cross-sections (parallel to grid mesh) where the analysis of salt flux decomposition is carried out. The arrows point to the three estuaries.

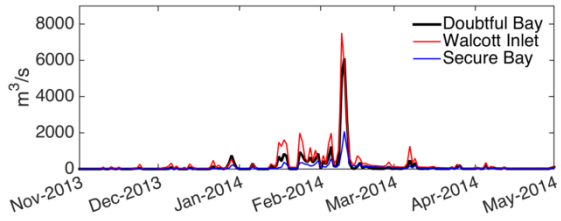

Figure 2. Total river runoff at Collier Bay. There are three estuaries that flow into Collier Bay (Figure 1): Doubtful Bay, Walcott Inlet (Isdell river) and Secure Bay.

Numerical simulation with ROMS

Hydrodynamic simulation with ROMS (Allen et al., 2003; Warner et al., 2005; Geyer and Lerczak; 2005) was carried out on the domain shown in Figure 1 from November 2013 to May 2014. The averaged horizontal resolutions of the domain are 660 m in the lateral and 535 m in the longitudinal, and 30 sigma-layers were configured in the vertical. Wind forcing was not applied in order to exclude the interference of wind-driven processes when analyzing salt fluxes with the simulation results. A large freshwater flow occurred during the simulation period (Figure 2), entering Collier Bay via the 3 estuaries (Figure 1).

ROMS was validated against sea surface height (SSH), temperature (T) and salinity data collected by the three moorings shown in Figure 1. ROMS captured the variations of SSH (data at the middle mooring has not been presented as the pressure sensor failed), temperature and salinity very well (Figure 3 and 4). In

particular, ROMS simulated the sharp drop of salinity (from about 34.5 psu to 29.8 psu) at the inner mooring due to the peak freshwater inflow into the bay, which matched well with the measurement (dropped from about 34. 8 psu to 29.1 psu). The statistics in Table 1 also confirmed that the temperature and salinity simulated by ROMS agreed well with the mooring measurements.

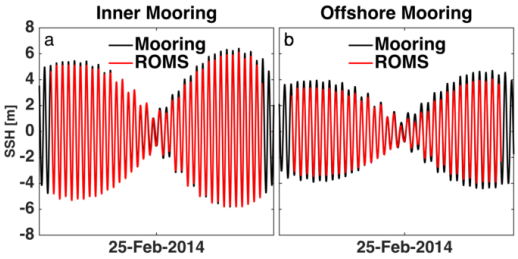

Figure 3. Sea surface heights simulated by ROMS (black) compared with measurements (red) during a wet season spring-neap cycle at (a) inner mooring and (b) offshore mooring.

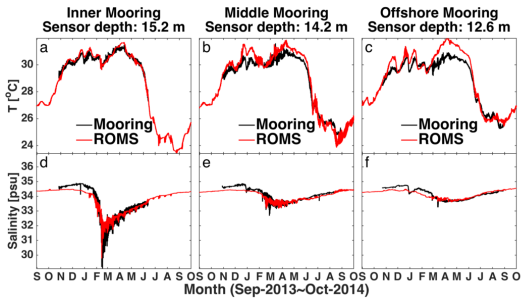

Figure 4. Temperature (upper panel) and salinity (lower panel) simulated by ROMS (black) compared with measurements (red) at the inner mooring (a & d), middle mooring (b & e) and offshore mooring (c & f).

		Inner	Middle	Offshore
Temperature	Centered RMS difference (℃)	0.201	0.421	0.466
	Correlation coefficient	0.966	0.991	0.979
Salinity	Centered RMS difference (psu)	0.305	0.154	0.174
	Correlation coefficient	0.980	0.957	0.891

Table 1. Model data agreement with field measurements at the three moorings, indicated by the centered Root Mean Square difference and the correlation coefficient.

ROMS was also validated with shipboard thermosalino-graph data (temperature and salinity) sampled at 2.8 m below the sea surface during a dry season cruise in October 2013 and a wet season cruise in March 2014 (not shown here), demonstrating that ROMS was able to reproduce the density field in both the dry and wet seasons, and in particular the salinity field in the wet season.

Salt flux decomposition

Mechanisms driving the salt flux include advection, steady shear dispersion and tidal oscillations (Lerczak et al., 2006). To distinguish the salt flux components driven by each of these mechanisms, Eulerian salt flux decomposition (Lerczak et al., 2006; MacCready, 2011) was applied:

$$F = FR + FE + FT = u_0 s_0 A_0 + \int u_1 s_1 dA_0 + <\int u_2 s_2 dA> \quad (1)$$

Where <> denotes a Godin-type low-pass filter; $\int$ denotes integration over the cross-section area; F is the total salt flux; FR, FE, FT are the advective, steady shear dispersion and tidal oscillatory salt flux, respectively; dA is the differential area element in the vertical; u_0, s_0, A_0 are the tidally and spatially averaged velocity, salinity and cross-sectional area that are calculated as:

$$u_0 = \frac{<\int udA>}{A_0},\ s_0 = \frac{<\int sdA>}{A_0},\ A_0 = <\int dA> \quad (2)$$

Variables u and s are the horizontal velocity and salinity output by ROMS. Note that A (or dA) is the cross-sectional area that calculated with depth without being filtered, so it varies with sea surface height. To the contrary, A_0, u_0, s_0 and thus FR are quantities with significant fluctuations due to sub-tidal variation of sea surface height excluded. Variables u_1, s_1 are the tidally averaged and sectionally varying horizontal velocity and salinity, and dA_0 is the tidally averaged differential area element:

$$u_1 = \frac{<udA>}{dA_0} - u_0,\ s_1 = \frac{<sdA>}{dA_0} - s_0,\ dA_0 = <dA> \quad (3)$$

The remainders are the tidally and sectionally varying horizontal velocity and salinity that are associated with the tidal oscillatory salt flux:

$$u_2 = u - u_0 - u_1,\ s_2 = s - s_0 - s_1 \quad (4)$$

As shown in Figure 1, the cross-sections are laterally parallel to the grid mesh of ROMS; therefore the horizontal velocity u, here and after, is the longitudinal velocity which is positive pointing towards the northwestern corner of the domain and negative towards the southeastern corner. Since the northeastern corner of the ROMS domain is the open ocean where salinity is high and the southeastern corner is influenced by river input resulting in lower salinity, the flux from northeast to southeast will be described as the downgradient direction and the opposite direction will be described as the upgradient direction. Thus the downgradient salt flux drives salt landward and the upgradient salt flux drives salt oceanward.

The Eulerian decomposition shows salt fluxes are driven by different mechanisms, but it does not provide further information about the upgradient flux or downgradient flux. Therefore, we also undertook an isohaline salt flux decomposition to characterize the upgradient and downgradient fluxes as functions of salinity (MacCready, 2011). Firstly, it defines the tidally averaged volume flux of water with salinity above a specific salinity s as

$$Q(s) = <\int_{A_s} udA> \quad (5)$$

Where A_s is the area of the portion of the cross-section with salinity above certain specific salinity s. Then the upgradient and downgradient fluxes are calculated as

$$-\frac{\partial Q}{\partial s} = -lim_{\delta s \to 0} \frac{Q\left(s+\frac{\delta s}{2}\right) - Q\left(s-\frac{\delta s}{2}\right)}{\delta s} \quad (6)$$

$$Q_{up/downgradient} = \int -\frac{\partial Q}{\partial s}|_{up/downgradient} ds \quad (7)$$

$$F_{up/downgradient} = \int s(-\frac{\partial Q}{\partial s}|_{up/downgradient}) ds \quad (8)$$

Here, $-\frac{\partial Q}{\partial s}$ is the differential isohaline volume flux (the volume flux at a specific salinity) and F is the salt flux. The flux-weighted salinities of the upgradient and downgradient fluxes are then calculated as

$$s_{up/downgradient} = \frac{F_{up/dwongradient}}{Q_{up/downgradient}} \quad (9)$$

Both the Eulerian decomposition and isohaline decomposition were carried out at the three channels and Walcott Inlet. Specific attention was paid to comparing North Channel and Walcott Inlet, as the bathymetry of the two regions consists of shallow and deep sections, but varies laterally at North Channel while longitudinally at Walcott Inlet.

Results and Discussion

The Eulerian decomposition reveals that the mechanisms driving the salt flux differed between North Channel and Walcott Inlet. At North Channel the advective salt flux was the dominant component and the other two Eulerian salt flux components were negligible (Figure 5, notice the different scales in the panels). In contrast, at Walcott Inlet the advective salt flux was the same order as the other two salt fluxes (Figure 6). Results of the isohaline decomposition (Figure 7 and 8) shows that at North Channel and Walcott Inlet, the variation of both the upgradient salt flux and downgradient salt flux was largely influenced by the freshwater inflow. At North Channel, the upgradient flux-weighted salinity varied at the same rate as the downgradient flux-weighted salinity, indicating a well-mixed condition in the channel. At Walcott Inlet, the upgradient flux-weighted salinity dropped much more dramatically than the downgradient flux-weighted salinity, indicating that the buoyancy introduced by the peak freshwater inflow was sufficient to maintain a strong vertically stratified condition at the estuary for that short period of time. The salinity at the cross section for the upgradient fluxes showed lower salinity because these fluxes are directed from the interior of the bay towards the open ocean.

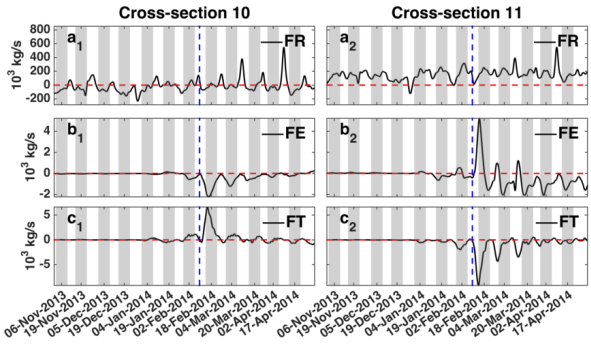

Figure 5. Eulerian salt flux components across cross-section 10 (left column) and 11 (right column) at North Channel. $a_{1,2}$: Advective salt flux (FR). $b_{1,2}$: Steady shear dispersion salt flux (FE). $c_{1,2}$: Tidal oscillatory salt flux (FT). Red dashed line indicates zero salt flux; blue dashed line indicates the date of the peak total river runoff (10-Feb-2014) as shown in Figure 2. Shaded panels (7 days in width) indicate spring tides.

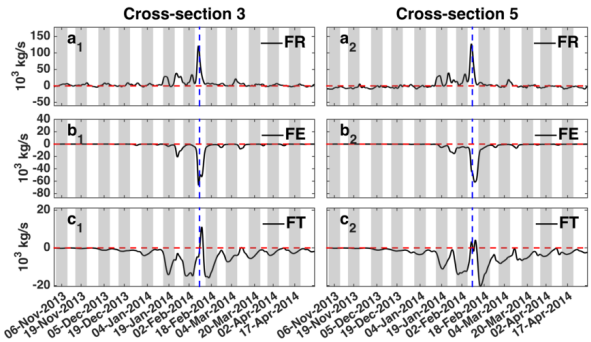

Figure 6. Eulerian salt flux components across cross-section 3 (left column) and 5 (right column) at Walcott Inlet (notations as in Figure 5).

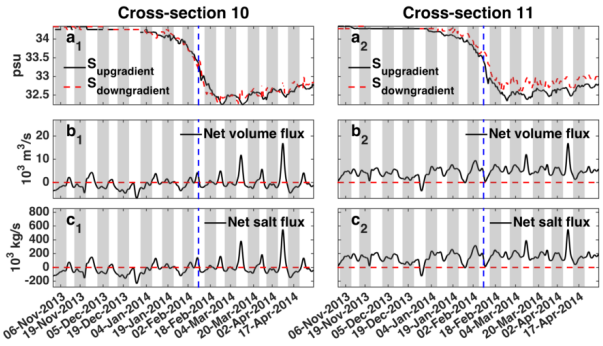

Figure 7. Isohaline salt flux components across cross-section 10 (left column) and 11 (right column) at North Channel. $a_{1,2}$: Flux-weighted salinity ($s_{up/downgradient}$). $b_{1,2}$: Net volume fluxes ($Q_{upgradient} - Q_{downgradient}$); $c_{1,2}$: Net salt fluxes ($F_{upgradient} - F_{downgradient}$). Blue dashed line indicates the date of the peak total river runoff (10-Feb-2014) as shown in Figure 2. Shaded panels (7 days in width) indicate spring tides.

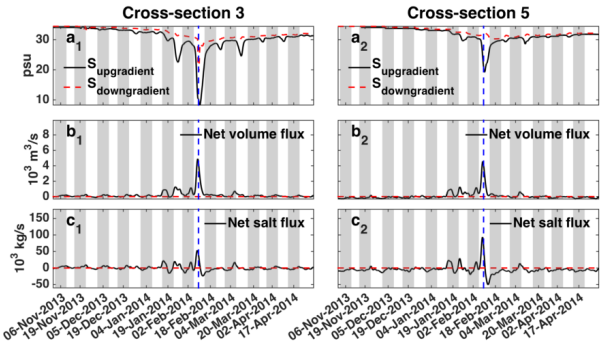

Figure 8. Isohaline salt flux components across cross-section 3 (left column) and 5 (right column) at Walcott Inlet (notations as in Figure 7).

North Channel is bordered by Montgomery Reef. To study the influence of this shallow region on exchange through North Channel we compared the salt flux across the deep part of the channel (cross-section 10, Figure 1) to a cross-section that extends further to include a shallow section over Montgomery Reef (cross-section 11, Figure 1). Firstly, Eulerian decomposition results at North Channel (Figure 5) show that the dominant advective salt flux at cross-section 10 (deep part of channel) fluctuated between upgradient (positive) and downgradient (negative); while the advective salt flux at cross-section 11 (including Montgomery Reef section) was generally upgradient throughout the entire wet season. The net salt fluxes derived from the isohaline decomposition concurred (Figure 7$c_{1,2}$). Secondly, directions of steady shear dispersion salt flux and tidal oscillatory salt flux at cross-section 10 were downgradient and upgradient, respectively, the reverse was observed at cross-section 11. Thirdly, although North Channel was well-mixed, as indicated by the upgradient and downgradient flux-weighted salinity at both cross-sections ($a_{1,2}$ in Figure 7), the difference between the upgradient and downgradient flux-weighted salinity at cross-section 11 was more evident than that at cross-section 10. In summary, freshwater and ocean water was not as well mixed in the shallow part of North Channel over Montgomery Reef, contributing to the upgradient net salt flux at North Channel.

In Walcott Inlet, the topography varies in the longitudinal direction, differing from that in North Channel. The Eulerian salt fluxes at the shallower cross-section 3 behaved similarly to those at the deeper cross-section 5 (Figure 6), but very differently from those at North Channel. As mentioned above, the advective salt

flux at Walcott Inlet was not a dominant component, but it was the major upgradient component. In contrast, both the steady shear dispersion salt flux and the tidal oscillatory salt flux were downgradient, with the exception that the latter reversed quickly during peak river runoff. The isohaline decomposition results show that periodic vertical stratification was established in Walcott Inlet as the upgradient flux-weighted salinity dropped more dramatically than the downgradient flux-weighted salinity ($a_{1,2}$ in Figure 8), especially when the estuary was flooded by the peak freshwater inflow. The net volume flux and net salt flux ($b_{1,2}$ and $c_{1,2}$ in Figure 8) indicated a general balance through the entire wet season, with only a sharp fluctuation towards upgradient fluxes due to the peak freshwater inflow. The stratification then weakened dramatically and the salt balance was quickly restored to a similar level prior to the peak freshwater inflow as the upgradient flux-weighted salinity started to increase immediately after the river inflow decreased.

Figure 9 compares the differential isohaline volume fluxes parameterized by Eq. 6 along the longitudinal-axis of Walcott Inlet on a spring tide and a neap tide after the peak freshwater inflow when the flow rate had greatly declined, representative of the majority of the wet season. On the spring tide, the differential volume flux with salinity below 28 was mostly trapped in Walcott Inlet, especially in the shallow part between cross-section 1 and 3. On the neap tide, there was a stronger upgradient volume flux from upstream of Walcott Inlet into Collier Bay, of which the salinity range varied between 22~26 and 29~31.5, indicating continuous mixing with ocean water along the path.

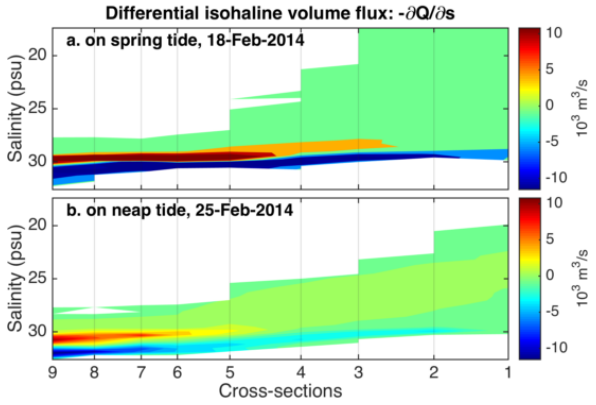

Figure 9. Differential isohaline volume fluxes ($-\frac{\partial Q}{\partial s}$) at Walcott Inlet tide after the peak inflow on (a) a spring tide and (b) a neap tide.

The net salt flux was different at each of the three channels connecting Collier Bay to the surrounding ocean (not shown). The net salt flux through the southern channel was downgradient, while the net salt flux through the other two channels was upgradient. The upgradient flux was stronger at North Channel than at the middle channel. Thus, Collier Bay received salt from the ocean through the southern channel while being diluted through the middle and North Channels. Note that the southern channel is the deepest among the three channels (Figure 1).

Conclusions

A ROMS simulation was used to analyze the salt fluxes at Collier Bay in the wet season. The model was found to perform well considering the unique context of the complex coastline shape, bathymetry and macro-tidal forcing. Salt flux components driven by different mechanisms (advection, steady shear dispersion and tidal oscillation) were obtained with the Eulerian salt flux decomposition method and complemented with information about the upgradient and downgradient salt fluxes using the isohaline salt flux decomposition method. Through the comparison of the dynamics at North Channel and Walcott Inlet, it is clear that bathymetric variation in different directions (lateral or longitudinal) has different impacts on the interaction between tides and freshwater inflow in shaping salt fluxes and thus the horizontal mass exchange. At North Channel, shallow flow in the lateral direction plays a significant role in the net salt flux. The longitudinal bathymetric variation had less impact on the Eulerian salt fluxes and the net salt flux, but had a significant impact on both the upgradient and downgradient components as shown for Walcott Inlet.

Future work will further analyze the variation in the advective salt flux at North Channel after the peak freshwater inflow has passed (Figure 5). Specifically, we will identify the mechanisms responsible for the much stronger upgradient salt flux on neap tides compared with the minimal downgradient salt flux on spring tides. Furthermore, we will identify the individual contributions of tidal pumping and tidal trapping to the tidal oscillatory salt flux. It is envisioned that the improved understanding of mass exchange within this environment will allow for improved predictions of sediment and nutrient transport processes.

Acknowledgments

The Western Australian Marine Science Institute (WAMSI) provided funding for this study through the Kimberly Marine Research Program projects 2.2.1 and 2.2.6.

References

[1]. Allen, S. E. et al., On Vertical Advection Truncation Errors in Terrain-Following Numerical Models: Comparison to a Laboratory Model for Upwelling over Submarine Canyons, Journal of Geophysical Research, **108**, 2003, C13003.

[2]. Cresswell, G. R. & Badcock, K. A., Tidal Mixing Near the Kimberley Coast of NW Australia, Marine Freshwater Research, **51**, 2000, 641-646.

[3]. Geyer, W. R. & Lerczak, J. A., Numerical Modeling of an Estuary: a Comprehensive Skill Assessment, Journal of Geophysical Research, **110**, 2005, C05001.

[4]. Jones, N. L. et al., Biophysical Characteristics of a Morphologically-Complex Macrotidal Tropical Coastal System During a Dry Season, Estuarine, Coastal and Shelf Science, **149**, 2014, 96-108.

[5]. Lerczak, J. A. et al., Mechanisms Driving the Time-Dependent Salt Flux in a Partially Stratified Estuary, Journal of Physical Oceanography, **36**, 2006, 2296-2311.

[6]. MacCready, P., Calculating Estuarine Exchange Flow Using Isohaline Coordinates, Journal of Physical Oceanography, **41**, 2011, 1116-1124.

[7]. Warner, J. C. et al., Performance of Four Turbulence Closure Models Implemented Using a Generic Length Scale Method, Ocean Modelling, **8**, 2005, 81-113.